Size Dependent Band Gap Properties of Silicon Nanocluster with Hydrogen and Oxygen Passivated At the Surface

A Graduate These Submitted To the School of Graduate Studies of Addis Ababa University. In partial Fulfillment of The Requirements For The degree of Masters of Science in physics.

By

Ermias Atnafu Abebe
Addis Ababa
Ethiopia
April 2007

ADDIS ABABA UNIVERSITY

SCHOOL OF GRADUATE STUDIES

By Ermias Atnafu Abebe

Department of Physics
Faculty of Science

Approved by the Examination Committee

Name	Signature
Advisor Dr. Ghoshal	_____
Examiner P. Singh	_____
Examiner Dr. Genene	_____

Acknowledgment

First and for most I would like to thank my God.

It is with great pleasure that I thank and acknowledge my advisor, Dr. Ghoshal, for his comments, suggestions and genuine advises he offered me during the progress of this work. His dedication, knowledge and skill as a qualified instructor and advisor are an inspiration. Thank you.

Thanks to Emiwodish my mama, all my brothers and sisters for all your heart full support in the process. I do not forget yours to Emuye (Tizi).

Thanks to the **Infonet college** management who gave me the chance to work and learn and all what you have done for me is beyond words to describe. Thank you Dr Nega. Thank you.

Abstract

Theoretical study of the electronic structure properties of silicon nanocluster (size ≤ 5 nanometer), in particular the role played by quantum confinement and hydrogen passivation have been studied using the empirical pseudo potential approximation method. We have calculated the gap energy of the nanocluster for different sizes between the highest occupied molecular orbital (HUMO) and the lowest unoccupied molecular orbital (LUMO). It is observed that quantum confinement effect plays the greatest role for HOMO LUMO gap difference i.e. as the number of atoms in the dot decreases; there is a considerable increase in the energy gap. Hydrogen passivation and addition of oxygen also widens the gap energy. We have compared our results with tight binding and other calculations. The agreement with other results confirms the validity of quantum confinement model gap enhancement that is responsible for visible luminescence in nanosilicon.

Table of Contents Pages

Acknowledgement iii
Abstract iV
Table Contents V
List of Tables Vi
List of figures Vii
Chapter One
1. Introduction
Chapter Two 10
2.0 . Quantum Confinement In Silicon Nano Cluster 10
2.1. Formulation of the Local Empirical Pseudopotential Method. 12
2.2. Electronic Structure Of Quantum Dots 16
2.3. Free Electron Gas 17
2.4. Boundary Conditions And Enumeration Of States 19
2.5. Empirical Pseudopotential Model 24
2.6. Numerical Method 26
Chapter Three 29
3.0 Result and Discussion
Chapter Four 40
4.0 Summary and Conclusion 41
References

Index 43

List of Tables Pages

Table 2.1. Matrix size for a fixed cell size=5.43 A^0 when the cutoff energy is varied. 22

Table 2.2. [Cell size is varied] fixed Ecut off=10 Ryd] 23

Table 2.3. For fixed effective size L and fixed cut off when the number of atoms in the dot is varied. 23

Table 2.4. Numerical results from our simulations. 28

Table 2.5. Our results for the gap energy as a function of the dot size 33

List of Figures Pages

Figure 1.1. Ground state geometries and some low-energy isomers of Si_n ($n \leq 7$). 2

Figure 1.2. Schematic of the direct and indirect band gap of semiconductors. 3

Figure 1.3. The increase of the band gap with decreasing crystalline size due to quantum confinement. 5

Figure 1.4. Hydrogen passivated silicon cluster. 7

Figure 2.1. Standard pseudopotential model of a solid. The ion cores composed of the nuclei and tightly bound core electrons are treated as chemically inert. The pseudopotential model describes only the outer chemically active valence electrons. 17

Figure 3.1. Plot of number of atom in the dot verses HOMO-LUMO energy gap value without any passivation. 34

Figure 3.2. Plot of number of silicon atoms in the dot verses HOMO-LUMO energy gap value with and without hydrogen passivation. 35

Figure 3.3. Plot of number of silicon atoms in the dot verses HOMO-LUMO energy gap value with oxygen and without any passivation. 36

Figure 3.4. Plot of number of silicon atoms in the dot verses HOMO-LUMO energy gap value with no passivation, with hydrogen and with oxygen passivation. 37

Figure 3.5. Plot of number of silicon atoms in the dot verses HOMO-LUMO energy gap value without passivation (our result and tight binding). 38

Figure 3.6. Plot of number of silicon atoms in the dot verses HOMO-LUMO energy gap value with hydrogen passivation (tight binding and ours). 39

Figure 3.7. Plot of number of silicon atoms in the dot verses HOMO-LUMO energy gap value with oxygen passivation (tight binding and ours). 40

Chapter One

Introduction

At present, there is a considerable interest in the potential use of materials with dimensions that are best defined in terms of nanometers [1]. Although research on nanocrystals started in the early eighties, the spectacular level of cavity was witnessed only in the nineties with the emergence of improved techniques for the synthesis of high quality nanocrystals and better instruments to characterize them [2].

A nanocrystal is a tiny chunk of the bulk measuring a few nanometers with a finite number of atoms in it. Nanocrystals poses high surface area. Large fractions of the atoms in nanocrystals are on the surface. A small nanocrystal of one nanometer diameter will have as much as 30% of its atoms on the surface while a larger nanocrystal of 10 nanometers (~1000 atoms) will have around 15% of its atoms on the surface.

The electronic, magnetic and optical properties of a nanocrystal depend on its size. In small nanocrystals, the electronic energy levels are not continuous as in the bulk but are discrete due to the confinement of the electron wave function to the physical dimension of the particle. If the size of the nanostructure become of the order of exciton Bohr radius quantum confinement is important and the energy level become discrete. This phenomenon is called quantum confinement and nanocrystals are known

as quantum dots (see figure 1.1). If the size of the nanostructure becomes of the order of exciton Bhor radius quantum confiment is important and the energy level becomes discrete. Most recently experimental evidences suggest that the strong photoluminescence in the visible region is due to the enhancement of the momentum matrix element associated with the quantum confinement of the electronic wave functions of silicon nanostructures or dots [1]. The other suggestion is that the surface chemical composition of silicon nanostructures may also play a key role in the enhanced photoluminescence [3].

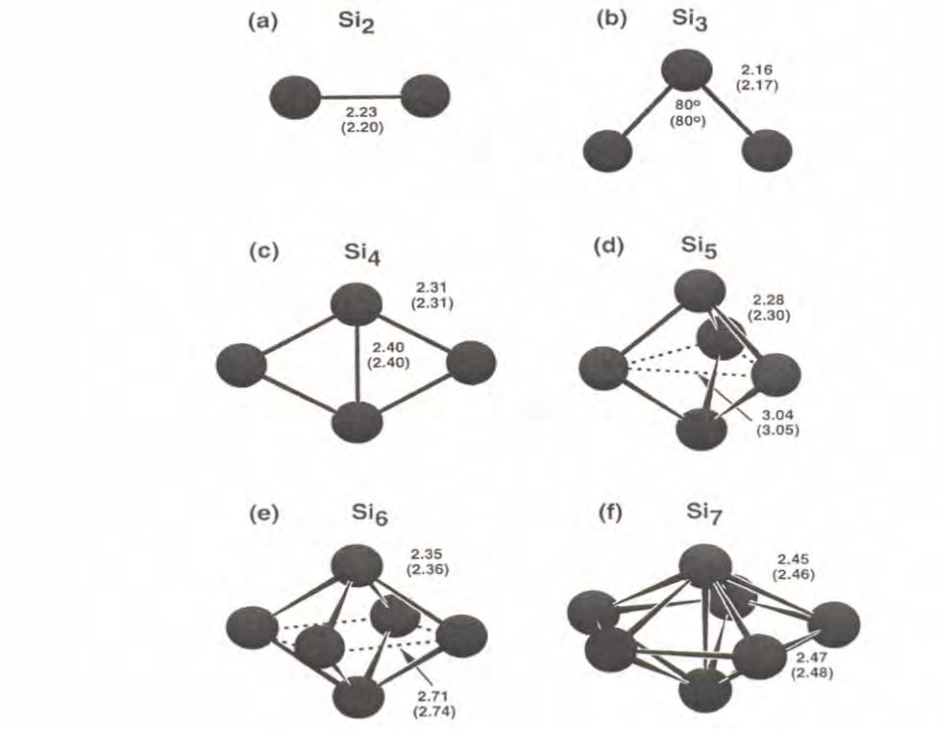

Figure 1.1. Ground state geometries and some low-energy isomers of Si_n ($n \leq 7$).

A great deal of effort has been devoted to study the size dependence of the gap of silicon quantum dots. Though bulk silicon is an indirect band gap semiconductor (see figure 1.2), quantum confinement in nanocrystaline silicon modifies the bulk silicon band structure from an indirect to direct band gap [4]. It is generally accepted that the quantum confinement effect in the nanocrystalities opens up the band gap as well as relaxes the selection rule for irradiative transitions giving rise to the above band gap photoluminescence in the visible regime for crystallite size below 10 nanometers [3].

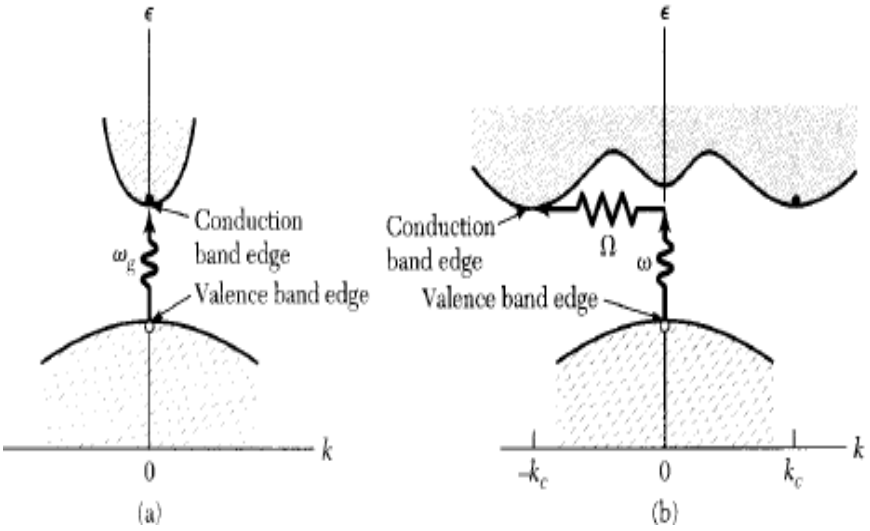

Figure 1.2. Schematic of the direct and indirect band gap of semiconductors.

The quantum confinement alone cannot explain the role played by various surface treatments in the surrounding media. The participation of the localized surface states or defects in oxides had been suggested to influence the photoluminescence peak

energy and line shape. These localized states induced by the atomic disorder (structural or compositional) exist at the surface of nanocrystalities and are energetically placed within the band gap [5].

Experimentally it is difficult to control the number of atoms in silicon nanocluster. Hence, in most cases the experimental fabricated samples will not possess an overall symmetry. This brings the question: can a general clusters with an overall symmetry exhibit a wide and clean energy gap. The other issue is related to the size dependency of the gap of a general cluster (see figure 1.3) [3]. A nanocluster left to itself will search for a stable configuration by relaxation and surface reconstruction. The process is triggered by the tendency of the cluster to minimize its total energy [1]. This causes severe distortion of the bonds in particular of the exterior atoms. This reconstruction leads to the reduction of surface dangling bonds. However, it may not eliminate the dangling bonds on the surface. Hence, there will also be defect states associated with the remnant dangling bonds. These defect states may fall in the gap region making the gap less clean or even dirty [1]. The bonding configurations of the interior atoms are bulk like and the surface feature exhibits the characteristics of the most stable surface reconstruction of Si. However, the bonding configurations of the exterior atoms show more sever distortions from the regular tetrahedral network as the size of the cluster decreases [6].

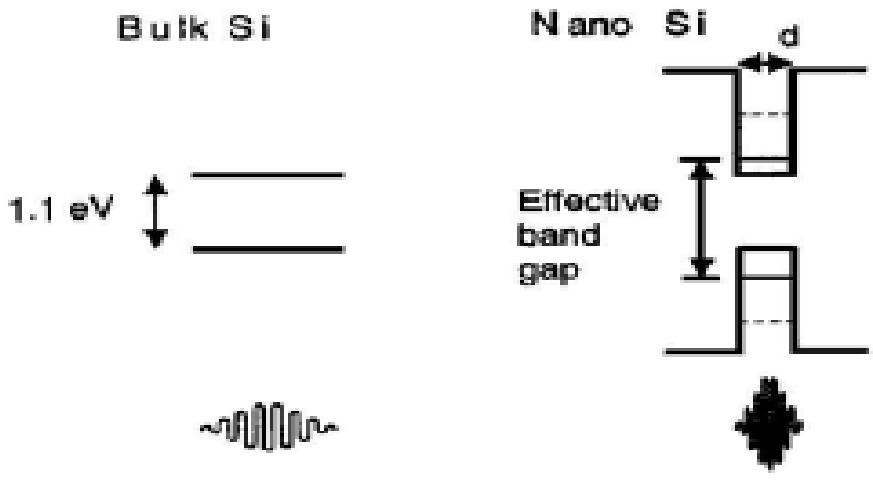

Figure 1.3. The increase of the band gap with decreasing crystalline size due to quantum confinement.

Dangling bonds could be removed from the dot by passivation with hydrogen (see figure 1.4). Experimental investigations indicates that the presence of hydrogen at the surface contributes surface states near the gap to enhance the gap energy and hence the confinement [7]. One may produce a cluster with a well-defined clean gap by passivating unrelaxed cluster with hydrogen or other appropriate atomic species regardless of the size of the cluster. But passivation must be completed before the cluster has the time or the opportunity to relax or the passivation is carried out through a combined process of annealing and passivation. The unrelaxed cluster is constructed by the following way: the silicon atoms are placed or distributed on the tetrahedral site

in a random manner. Hence, a cluster constructed in this way will have undistorted local bonding configuration. We passivated these dangling bonds associated with this unrelaxed configuration and the cluster posses a clean and a much wider gap than the nonpassivated cluster.

Relaxation ensures that the cluster is in a stable configuration. Although the relaxation process can eliminate dangling bond states, it is found that this process introduces impurity states in the gap associated with the bond distortion of surface atoms in the cluster. These impurity modes cannot be eliminated by further saturation of remnant dangling bonds with hydrogen. The relaxed hydrogen passivated silicon nanocluster with no bond distortion has the cleanest energy gap and the most stable structure among the different cases studied [3].

The structural properties of hydrogenated silicon nanocrystals have little effect, contrary to their electronic properties. The surface relaxation is quit small in the hydrogen-saturated Si nanocrystals, with lattice cons traction of 0.01-0.02 A^0 . Within the outermost two or three layers. Inside the hydrogenated Si nanocrystals, there is only a very small strain (lattice expansion) of the order of 10^{-4}-10^{-3}. The fully hydrogenated Si nanocrystals are the most stable structures compared to partially hydrogenated ones.

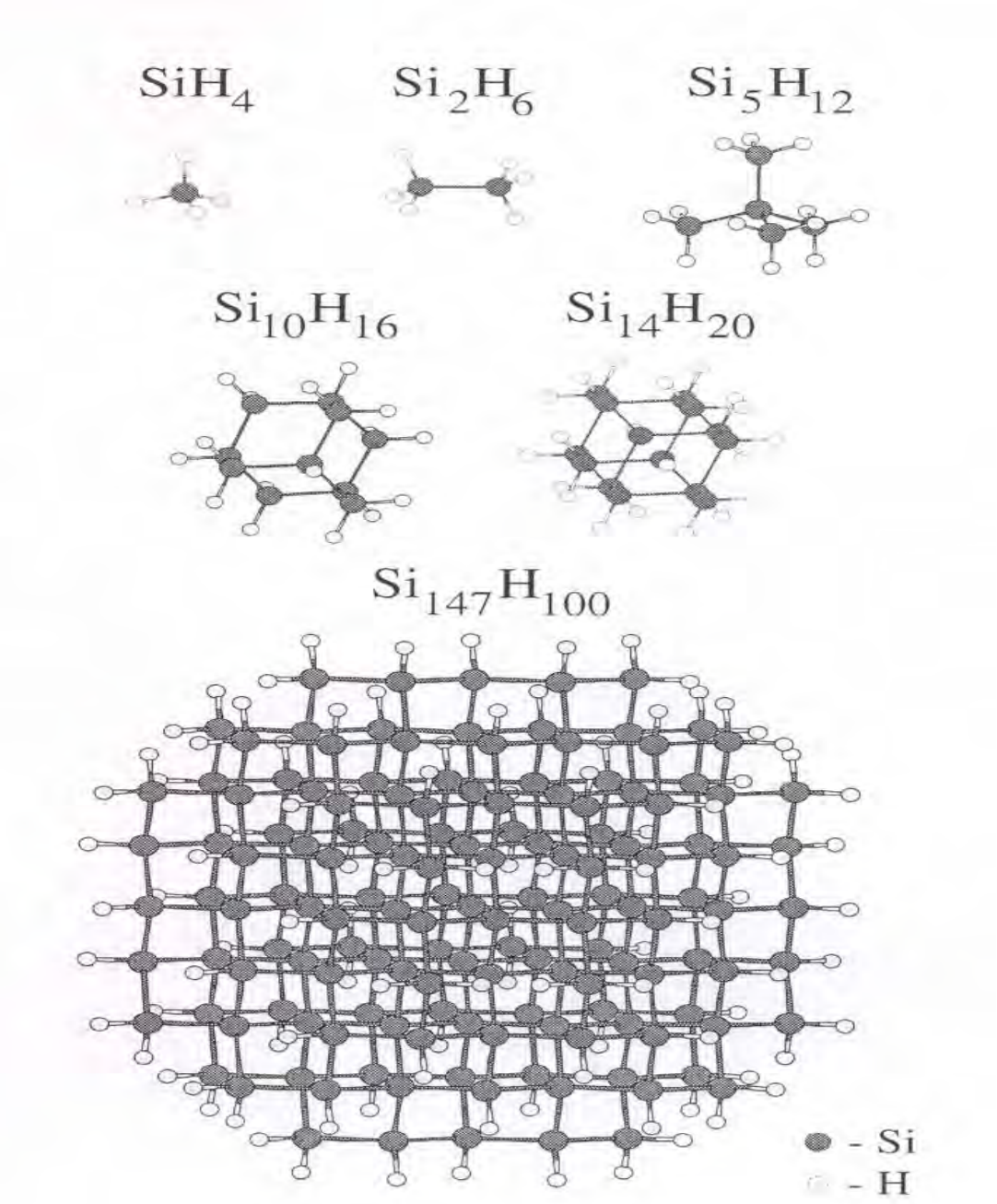

Figure 1.4. Hydrogen passivated silicon cluster.

The electronic and optical properties of silicon nanocrystal are likely to be affected by surface passivation because the majority of silicon atoms in the silicon nanocrystals are on or near the surface. Thus, understanding and controlling surfaces would be particularly important in silicon nanocrystals especially for their optoelectronic application [9].

When porous Si is exposed to air oxygen as expected to play a key role on the surface of porous Si and some oxidation, induced electronic states would be involved in the recombination of electrons and holes in quantum confined silicon nanocrystals. The occurrence of these oxidation-induced states especially near the energy gap would depend on the configuration of oxygen on the surface of a Si nanocrystal [10].

Oxidized clusters were prepared from regular hydrogen-terminated spherical dots by replacing two hydrogen atoms on the surface with a single atom of oxygen, followed by relaxation of all inter atomic forces. The addition of oxygen creates new absorption bands in the region of lower transition energies.

Since the gaps in silicon dots decreases with increasing cluster size because of diminishing quantum confinement, at some point the oxygen-induced states are expected to cross over the electronic levels from the body of the cluster. After this point, the oxygen-induced states would no longer be localized inside the gap. Calculations suggest that depending on the fraction of oxygen coverage, the oxygen-induced states should not cross over the levels from the body of the cluster for silicon

dots up to approximately 20-25 A^0. in diameter [9]. For larger dots, the over all effect of surface oxidation on the optical properties is likely to be less important.

The aim of my thesis is to investigate the dependence of the energy gap between the conduction and valence band in the cluster on the size of the dot, the effect of the passivated hydrogen and oxygen on the surface.

The remaining part of this thesis is organized as follows. In chapter two, we will see the model in detail and using the empirical pseudopotential Hamiltonian and a plane wave basis expansion and a basic tetrahedral structure we will discuss the dependence of the energy gap and gap states on size of Si dots. The effect of passivation of the surface dangling bonds by hydrogen atoms and the role of the surface states on the gap energy as well as the HOMO (highest occupied molecular orbit) LUMO (lowest unoccupied molecular orbit) states has also examined in detail.

In chapter three, we will present result and discussion and the last and the fourth chapter will hold the summary and conclusion.

Chapter Two

2.0. Quantum Confinement in Silicon Nanocluster

The change in the electronic structure of nanomaterials as one change the size of the crystallites can be understood as a particle in a box like problem. Where, the energy level spacing increases as the box dimensions are reduced due to quantum confinement. The quantum confinement effect changes the energy level continuum in the bulk material in to a discrete level structure, namely the subband structure.

In the present work, we investigate the effect of quantum confinement on the energy gap states in silicon dots using the empirical pseudopotential Hamiltonian, a plane wave basis states and a basic tetrahedral structure. To understand the electronic property of silicon nanostructure in particular the role played by the surface, we examine the entire energy spectrum starting from the very low-lying ground state to the very high lying exited states for silicon dots having 2 to 40 atoms.

2.1. Formulation of the Local Empirical Pseudopotential Method.

The pseudopotential model of a solid has led the way in proving a workable model for computing the electronic property of materials [10]. For example, it is now possible to predict accurately the property of complex systems such as quantum dots or semiconductors, with hundreds or thousands of atoms.

The pseudopotential model treats matter as a sea of valence electrons moving in a background of frozen ion cores (see figure 2.1). The cores are composed of nuclei and inert inner electrons. Within this model, many of the complexities of all-electron calculations are avoided. For example, a group-IV solid such as C with six electrons is treated in a similar fashion to lead with 82 electrons.

Pseudopotential calculations center on the accuracy of the valence electron wavefunctions in the spatial region away from the core. That is with in the chemically active bonding region the smoothly varying pseudo wavefunctions is taken to be identical to the appropriate all-electron wavefunction in the bonding region. Therefore, we will begin by expanding the wavefunction with two separate terms, one representing the valence states in terms of plane waves $\sim e^{ik.r}$ and another representing the core states with an expansion of the eigen states of atomic core electrons $\psi(r)$.

The pseudopotential approximation exploits this by the following way: the core wavefunctions are well localized about the lattice sites. The valence electrons on the other hand can be found with appreciable probability in the interestial region. Where our hope is that their wavefunctions will be well approximated by a very small number of plane waves.

The difficulty with approximating valence wavefunctions by a few plane waves everywhere in space is that this hopelessly fails to produce the rapid oscillatory behavior required in the core region.

Consider a free electron plane state, the exclusion principle require that the free electron states be orthogonal to the atomic core state. The core states are highly localized orbital and the orthogonal requirement introduces many new oscillations into the plane wave states in the region of the atomic core. Since the kinetic energy of a state is proportional to the second derivatives of the wavefunctions the kinetic energy of the free electrons state is increased in the vicinity of the atomic core.

This could be taken care of by using not simple plane waves but plane waves orthogonalized to the core level right from the start. Thus, we define the orthogonalized plane waves by:

$$\varphi_k = e^{ik.r} + \sum_c b_c \psi_k^c(r); \text{ The subscript c stands for the core.} \quad (2.1)$$

The sum is overall core levels with Bloch wavefunctions are assumed to be known and the constant b_c is determined by requiring that φ_k be orthogonal to every core level.

Note that φ_k is also orthogonal to ψ_k^c.

$$\int dr\, \psi_k^{c*}(r)\varphi_k(r) = 0. \quad (2.2)$$

Substituting (2.1) into (2.2) yields

$$\int dr\, \psi_k^{c*}(r)\left(e^{ik.r} + \sum_c b_c \psi_k^c(r)\right) = 0. \quad (2.3)$$

We can expand this to:

$$\int dr\,\psi_k^{c*}(r)e^{ik.r} + \int dr\,\psi_k^{c*}(r)\sum_c b_c\psi_k^c(r) = 0 \tag{2.4}$$

$$\int dr\,\psi_k^{c*}(r)e^{ik.r} + \int dr\sum_c b_c\psi_k^{c*}(r)\psi_k^c(r) = 0 \tag{2.5}$$

From the normalization condition,

$$\int dr\,\psi_k^{c*}(r)e^{ik.r} + b_c = 0\,. \tag{2.6}$$

Therefore,

$$b_c = -\int dr\,\psi_k^{c*}(r)e^{ik.r}\,. \tag{2.7}$$

φ_k Has the following properties characteristic of valence level wavefunctions.

By explicit construction, it is orthogonal to all the core levels. It also has the required rapid oscillations in the core region. Since the core wavefunctions, $\psi_k^c(r)$ appearing in φ_k them selves oscillates in the core region.

Because the core levels are localized about lattice points, the second term is small in the interestial region where φ_k is very close to the single plane wave $\sim e^{ik.r}$.

Since the plane wave $e^{ik.r}$ and the core wavefunction $\psi_k^c(r)$ satisfy the Bloch condition with wavevector **k** so will the orthogonalized plane wave φ_k.

The actual electronic eigenstates of the Schrödinger equation is a linear combination of φ_k.

Let $\phi_k^v(r) = \sum_k c_k e^{i(k+G).r}$ the plane part of the expansion. (2.8)

Therefore,

$$\psi_k^v(r) = \phi_k^v(r) + \sum_c b_c \psi_k^c(r). \quad (2.9)$$

Substituting equation (2.7) into (2.9) yields,

$$\psi_k^v(r) = \phi_k^v(r) - \sum_c \left(\int dr' \psi_k^{c*}(r') e^{ik.r} \right) \psi_k^c(r), \quad (2.10)$$

$$\psi_k^v(r) = \phi_k^v(r) - \sum_c \left(\int dr' \psi_k^{c*}(r') \phi_k^v \right) \psi_k^c(r). \quad (2.11)$$

Since $\psi_v^v(r)$ is an exact valence wavefunction it satisfies Schrödinger equations with eigenvalues ϵ_k^v.

$$H\psi_k^v = \in_k^v \psi_k^v. \quad (2.12)$$

Substituting (2.11) into (2.12) yields,

$$H\left(\phi_k^v(r) - \sum_c \left(\int dr' \psi_k^{c*}(r) \phi_k^v(r) \right) \psi_k^c(r) \right)$$

$$= \in_k^v \left(\phi_k^v(r) - \sum_c \left(\int dr' \psi_k^{c*}(r) \phi_k^v(r) \right) \psi_k^c(r) \right). \quad (2.13)$$

$$H\phi_k^v - \sum_c \left(\int dr' \psi_k^{c*}(r) \phi_k^v(r) \right) H\psi_k^c = \in_k^v \left(\phi_k^v - \sum_c \left(\int dr' \psi_k^{c*} \phi_k^v \right) \psi_k^c \right). \quad (2.14)$$

Further rearrangement gives,

$$\mathrm{H}\phi_k^v = \sum_c \left(\int dr' \psi_k^{c*} \phi_k^v\right) H\psi_k^c + \in_k^v \left(\phi_k^v - \sum_c \left(\int dr' \psi_k^{c*} \phi_k^v\right)\psi_k^c\right). \tag{2.15}$$

From (2.12) and further expansion yields,

$$\mathrm{H}\phi_k^v = \sum_c \left(\int dr' \psi_k^{c*} \phi_k^v\right) \in_c \psi_c^k + \in_k^v \phi_k^v - \in_k^v \sum_c \left(\int dr' \psi_k^{c*} \phi_k^v\right)\psi_k^c \tag{2.16}$$

Rearranging (2.20) gives,

$$\mathrm{H}\phi_k^v = \sum \left(\in_c - \in_k^v\right)\left(\int dr' \psi_k^{c*} \phi_k^v\right)\psi_k^c + \in_k^v \psi_k^v, \tag{2.17}$$

$$\mathrm{H}\phi_k^v + \left(\in_k^v - \in_c\right)\left(\int dr' \psi_k^{c*} \phi_k^v\right)\psi_k^c = \in_k^c \phi_k^v, \tag{2.18}$$

$$\mathrm{H}\phi_k^v + V^R \psi_k^c = \in_k^v \phi_k^v. \tag{2.19}$$

Where; $V^R = \left(\in_k^v - \in_c\right)\left(\int dr' \psi_k^{c*} \phi_k^v\right)$.

$$\text{And} V^R \psi = \sum_c \left(\in_k^v - \in_c\right)\left(\int dr' \psi_k^{c*} \psi\right)\psi_k^c. \tag{2.20}$$

Therefore,

$$H + V^R = -\frac{\hbar^2}{2m}\nabla^2 + V^{PSEDO}. \tag{2.21}$$

The pseudopotential is defined to be the sum of the actual periodic potential U and V^R. For the potential, which is sufficiently small, we consider a nearly free electron calculation for the valence levels. Since the valence energies lies above the core energies, this is always positive. This leads the pseudopotential approximation to allow the wave function to be expanded using a small number of plane basis states by

removing the core electrons and by replacing them and the strong ionic potential by a weaker pseudo wavefunction rather than the valence wavefunction.

2.2. Electronic Structure of Quantum Dots

The actual geometry the cluster could be very much different (disc, cube, sphere, etc.) from these cube is chosen in this calculation. We have calculated the effective size of the dot using the expression,

$d\ (N) = \left(\frac{3}{4\pi\rho} \right)^{\frac{1}{3}} N^{\frac{1}{3}}$. Used by Wang and Zunger for the effective size of silicon atom.

We have also used the same formula in our approximation for the dot size. Where, N is the number of Si atoms in the dot and ρ is the mass density of bulk Si $\approx$ 2330 kg /m^3 at room temperature.

$d\ (N) = 3.3685\ N^{\frac{1}{3}}\ A^0$.

It follows that a dot with five atoms has diameter $\approx 5.8A^0$. These small-sized clusters have properties depending strongly on their size. One atom more or less may have a pronounced effect on the cluster's electronic structure. Therefore, the energy gap can strongly differ for clusters of similar size.

2.3. Free Electron Gas

Perhaps the simplest description of a condensed matter system is to imagine non-interacting electrons as contained with in a box of volume V. The Schrödinger equation for this is by setting the potential zero. For nearly free valence electrons,

$$H = \frac{P^2}{2m} = \frac{-\hbar^2 \nabla^2}{2m} \tag{2.22}$$

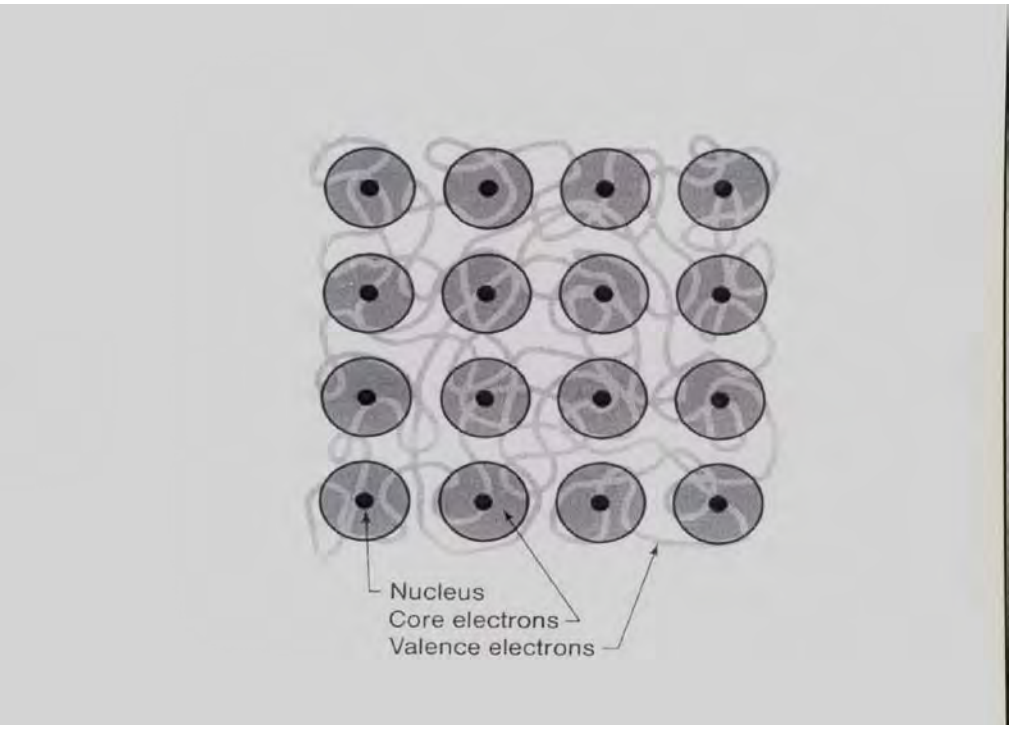

Figure 2.1. Standard pseudopotential model of a solid. The ion cores composed of the nuclei and tightly bound core electrons are treated as chemically inert. The pseudopotential model describes only the outer chemically active valence electrons.

Suppose the particle is confined within a container of volume V within which the particle is subjected to no force. Neglecting for the time being the effect of the bounding walls the wave functions $\psi(r,t)$ of the particle is then simply described by a plane wave of the form,

$$\psi = e^{i(k.r-wt)}\,\varphi(r)e^{-iwt}\,. \tag{2.23}$$

This propagates in a direction specified by the wavevector **k** and which has some constant amplitude A. Hence, the energy $\in$ of the particle is related to the frequency ω by $\in = \hbar\omega$.

While its momentum is related to the wavevector **k** by the de Broglie relation P= $\hbar k$.

$$\text{Thus, } \varepsilon = \frac{p^2}{2m} = \frac{\hbar^2 k^2}{2m}. \tag{2.24}$$

ψ Must satisfy the Schrödinger equation i $\hbar \frac{\partial \psi}{\partial t}$ =H ψ .

Since one can choose the potential energy to be zero inside the container. The Hamiltonian H reduces free to the kinetic energy alone.

$$\text{H}= \frac{p^2}{2m} = \frac{1}{2m}\left(\frac{\hbar\nabla}{i}\right)^2 = \frac{-\hbar^2\nabla^2}{2m} \tag{2.25}$$

$$\text{Where } \nabla^2 = \frac{\partial^2}{\partial x^2} + \frac{\partial^2}{\partial y^2} + \frac{\partial^2}{\partial z^2} \tag{2.26}$$

Putting $\psi = \varphi e^{-i\omega t} = \varphi e^{-\left(\frac{i}{\hbar}\right)\in t}$ (2.27)

Where ψ does not depend on the on the time reduces to the time independent Schrödinger equation.

$$H\psi = \in \psi \,. \tag{2.28}$$

Using equation (2.28),

$$\nabla^2\psi + \frac{2m \in}{\hbar^2}\psi = 0. \tag{2.29}$$

$\in$ Corresponds to the possible values of H and is thus the energy of the particle. Thus, the wave equation has solution of the general form

$$\psi = Ae^{i\left(k_x x + k_y y + k_z z\right)} = A\, e^{ik.r} \,. \tag{2.30}$$

Inserting (2.32) into (2.33) result in,

$$-\left(k_x^2 + k_y^2 + k_z^2\right) + \frac{2m \in}{\hbar^2} = 0 \,. \tag{2.31}$$

And solving for $\in$ results in ,

$$\in = \frac{\hbar^2 k^2}{2m} \,. \tag{2.32}$$

2.4. Boundary Conditions and Enumeration of States

The wave function ψ must be satisfying certain boundary conditions. The simplest boundary conditions to impose are such that a traveling wave of the form $\chi = \alpha e^{-i\omega t}$ in an exact solution of the problem. This requires that the wave be able to

propagate indefinitely with out suffering any reflections. In order to make the boundary conditions consistent with the simple situation one can neglect completely the presence of any container walls and can imagine that the volume of gas under consideration is embedded in an infinite of similar volumes in each of which the physical situation is the same. The wavefunctions must then satisfy the conditions.

$$\begin{aligned}\chi(x+l_x, y, z) &= \chi(x, y, z)\\ \chi(x, y+l_y, z) &= \chi(x, y, z)\\ \chi(x, y, z+l_z) &= \chi(x, y, z)\end{aligned} \tag{2.33}$$

Traveling wave described and going around with out reflection are perfectly good solution of the problem. It is only necessary to note that the points x and $x+l_x$ are now coincident the requirement that the wave function be single-valued implies the condition.

$$\chi(x+l_x)\chi(x)$$

$$k_x(x+l_x) = k_x x + 2\pi n_x \text{ ;(} n_x \text{ is an integer)} \tag{2.34}$$

Or $k_x = \dfrac{2\pi}{l_x} n_x$

$$k_y = \frac{2\pi}{l_y} n_y$$

$$k_z = \frac{2\pi}{l_z} n_z$$

Hence, n_x, n_y, and n_z are any set of integers positive or negative.

The components of x= $\frac{p}{\hbar}$ are thus quantized in discrete units. Accordingly

$\in = \frac{p^2}{2m} = \frac{\hbar^2 k^2}{2m}$ yields the possible quantized particle energies,

$$\in = \frac{\hbar^2}{2m}\left(k_x^2 + k_y^2 + k_z^2\right) = \frac{2\pi^2\hbar^2}{m}\left(\frac{n_x^2}{l_x^2} + \frac{n_y^2}{l_z^2} + \frac{n_z^2}{l_z^2}\right). \quad (2.35)$$

$$\text{Therefore, } \in = \frac{h^2}{2m}\left(\frac{n_x^2}{l_x^2} + \frac{n_y^2}{l_y^2} + \frac{n_z^2}{l_z^2}\right). \quad (2.36)$$

We have used two values of cutoff energy 5 Ryd and 10 Ryd to calculate the number of basis states.

For simplicity, we take $n_x = n_y = n_z$.

And $l_x = l_y = l_z$.

$$\text{Therefore, } \in = \frac{6\pi^2\hbar^2}{m}\left(\frac{n^2}{l^2}\right) = \frac{6\pi^2\hbar^2 n^2}{ml^2} = \frac{3h^2 n^2}{2ml^2}. \quad (2.37)$$

$$\text{We have set the cutoff as } \in_{cutoff} = \frac{h^2}{2m}\left(\frac{n_x^2}{l_x^2} + \frac{n_y^2}{l_y^2} + \frac{n_z^2}{l_z^2}\right). \quad (2.38)$$

We used two values of cutoff energy 5 Ryd and 10 Ryd to calculate the number of basis states.

For simplicity we take $n_x = n_y = n_z$, and $l_x = l_y = l_z$.

$$\in = \frac{6\pi^2\hbar^2}{m}\left(\frac{n^2}{l^2}\right) = \frac{6\pi^2\hbar^2 n^2}{ml^2} = \frac{3h^2n^2}{2ml^2}. \qquad (2.39)$$

Our interest is to find the size dependence of the gap energy and the near band gap solution. That is the separation between the highest occupied molecular orbital (HOMO) and the lowest unoccupied molecular orbital (LUMO). Now let us calculate the number of basis states for various $\in_{cutoff}$ values and then solve the effective single particle Schrödinger equation.

Table 2.1. Matrix size for a fixed cell size=5.43 A^0 when the cutoff energy is varied.

E_{cutoff} (Ryd)	**n**	**G's**	$G_x * G_y * G_z$	**N*N (Size of the matrix)**
5	± 2	$\pm 2, \pm 1, 0$	5*5*5	125*125
10	± 3	$\pm 3, \pm 2, \pm 1, 0$	7*7*7	343*343
15	± 4	$\pm 4, \pm 3, \pm 2, \pm 1, 0$	9*9*9	729*729
20	± 5	$\pm 5, \pm 4, \pm 3, \pm 2, \pm 1, 0$	11*11*11	1331*1331

Table 2.2. [Cell size is varied] fixed Ecut off=10 Ryd]

cell size in(A^0)		**G'S**	$G_x * G_y * G_z$	**N*N**
2	± 1	$\pm 1,0$	3*3*3	125*125
5.43	± 3	$\pm 3, \pm 2, \pm 1,0$	7*7*7	343*343
10	± 6	$\pm 3, \pm 2, \pm 1,0$	13*13*13	729*729
15	± 8	$\pm 8,\ldots, \pm 0$	17*17*17	1331*1331
20	± 11	$\pm 11,\ldots ,0$	23*23*23	12167*12167
25	± 13	$\pm 13,\ldots ,0$	27*27*27	19683*19683

Table 2.3. For fixed effective size L and fixed cut off when the number of atoms in the dot is varied

Number of atoms	**Matrix size N*N**
8	343*343
20	1331*1331
50	2197*2197
100	4913*4913
500	12167*12167
1000	166375*166375

2.5. Empirical Pseudo Potential Model

Once the number of basic states for a given fixed E_{cutoff} and effective size of the dot has been determined the next task is to solve the resulting eigenvalue problem needs to be solved for the system of interest.

Where $H = -\frac{1}{2}\nabla^2 + V(r)$ and $V(r)$ is the Fourier transform of $V_{Si}(G)$ given by $V_{Si}(q) = \frac{a_1(q^2 - a_2)}{a_3 e^{a_4 q^2 - 1}}$ (2.40)

Where $a_1 = 0.2685$, $a_2 = 2.19$, $a_3 = 2.06$, $a_4 = 0.487$ in the atomic unit (Hatree for energy Bohr for momentum q) these parameters are obtained by fitting the potential with bulk structure also from first principle calculations.

The hydrogen empirical pseudo-potential in atomic unit is given by

$V_H(q) = -0.1416 + 0.009802q + 0.0231q^2 - 0.01895q^3$; when $q \leq 2$

And, $V_H(q) = +\frac{0.02898}{q} - \frac{0.3877}{q^2} + \frac{0.9692}{q^3} - \frac{1.022}{q^4}$ when q>2.We used an ideal unrelaxed structure with Si-H bond distance of 1.487 A^0 and for Si-O_2 1.6-1.8 A^0.

The dot wave functions are expanded in a large basis of plane waves as

$\psi(r) = \sum_{Gj} B_j(G) e^{iG.r}$; G is the reciprocal vector B_j (G) are the expansion coefficients. Here $G_x = \frac{2\pi n}{l_x}$ etc. Where n_i are integers and l_x is the bond length (distance between two atoms) and B_{Gj} are the expansion coefficients to be determined variationally (minimizing the expectation value of the function H). We use different values of the cutoff energy for the plane wave expansion and the same cutoff is used for the potential energy too.

Knowing a set of values Gj values and corresponding initial guess values of ($B_{G1}, B_{G2}, B_{G3}, ...B_{Gn}$) now we minimize the expectation value of the function H .

$$< \psi_i \left| \overrightarrow{H} \right| \psi_i > \geq \hbar$$

With respect to the coefficients B_{Gj} 's subject to the normalization constraints

$$\sum_{Gj} \left| B_{Gj} \right|^2 = 1$$

Where λ_0 is some upper bound of the function after simplification we get an equation as a function of a B_{Gj} 's and Gj 's

$$< \psi_i \left| \overrightarrow{H} \right| \psi_i > = F(B_{G1}, B_{G2}, B_{G3}, ...B_{Gn}) \qquad (2.41)$$

$$< \psi_i \left| \overrightarrow{H} \right| \psi_i > = [G_1^2 \left| B_{G1} \right|^2 + G_2^2 \left| B_{G2} \right|^2 + ... + G_n^2 \left| B_{Gn} \right|^2]$$

$$+[V(G_1)|B_{G1}|^2 + V(G_2)|B_{G2}|^2 + ... + V(G_n)|B_{Gn}|^2] \qquad (2.42)$$

This should be minimized for a given initial choice of B_{Gj} say ($B_{G1}^0, B_{G2}^0, B_{G3}^0, ...B_{Gn}^0$) to be determined for a given set of Gj's say (G_1, G_2, … G_n) where the superscript zero represents the initial choice.

2.6. Numerical Method

For the minimization of the above function F ($B_{G1}, B_{G2}, B_{G3}, ...B_{Gn}$) we have used the conjugate gradient scheme to get its extremum value. Different set of choice of B_{Gj}'s will give different extreme values of the function starting from the lowest one. The lower most value of the function is the global minimum and all other higher values represent local minimum.

After minimization, we get the system of secular equations,

$$g_2^2 B_{g2} + 2V_{G1g2}B_{G1} + 2V_{G2g2}B_{G2} + ... + 2V_{Gng2}B_{Gn} = 0$$

$$g_1^2 B_{g1} + 2V_{G1g1}B_{G1} + 2V_{G2g1}B_{G2} + ... + 2V_{Gng1}B_{Gn} = 0$$

………………………………………………………..

……………………………………………………….. (2.43)

…………………………………………………………

$$g_n^2 B_{gn} + 2V_{G1gn}B_{G1} + 2V_{G2gn}B_{G2} + ... + 2V_{Gngn}B_{Gn} = 0 .$$

Where $V_{GG'}$ is given by $\int V(r)\exp(i(G-G').r)dr$ from these systems of equations we get the secular determinant to find out the eigenvalues.

$$\begin{pmatrix} (G_1^2\delta_{G1g1}+2V_{G1g1})(G_2^2\delta_{G2g1}+2V_{G2g1})..(G_n^2\delta_{Gng2}+2V_{Gng1}) \\ (G_1^2\delta_{G1g2}+2V_{G1g2})(G_2^2\delta_{G2g2}+2V_{G2g2})..(G_n^2\delta_{Gng2}+2V_{Gng2}) \\ ..... \\ ..... \\ ..... \\ (G_1^2\delta_{G1gn}+2V_{G+gn})(G_2^2\delta_{G2gn}+2V_{G2gn})..(G_n^2\delta_{Gngn}+2V_{Gngn}) \end{pmatrix} \begin{pmatrix} B_{G1} \\ B_{G2} \\ .. \\ .. \\ .. \\ B_{Gn} \end{pmatrix} = 0 \qquad (2.44)$$

We use different parts of the subroutine taken from the book numerical recepies by press [11].

The Hamiltonian matrix corresponding to the N atom dot can be written and the eigenvalues computed. For larger dots, the present method is not computationally efficient and is also time consuming as the size of the matrix increases rapidly as we increase the basis states for the larger dots. The aim is to look at how the band gap is sensitive to the surface effects and shapes of dots in order to examine the possible origin of photoluminescence due to the quantum confinement in the near surface region. We find all eigenvalues by direct dignalization method. After generating the matrix (N*N) we have found eigenvalues by directly diagonaizing the matrix using the standard subroutines. We use the numerical recipes FORTRAN code BALANCE.F to reduce it to Heisenberg form ‘ELMHES.F for the reduction Heisenberg form by the elimination method and HQR.F to find the eigenvalues of an

(N, N) upper Heisenberg matrix. The transformation between $\psi_j(r)$ on real space grid is done by numerical Fast Fourier transform (FFT). Even for a matrix of size (2000*2000) it becomes very much time expensive. It is not possible to handle the digitalization method for a matrix having size more than (1400*1400) with the help of the above subroutines. We present here the numerical results from our simulations of the model contained in equation (2.44) for the following dots.

Table 2.4. Numerical results from our simulations.

Effective size in (A^0)	**Number of atoms per dot**	**our: without hydrogen passivation, Eg(eV)**	**our: with hydrogen passivation, Eg(eV)**	**our: with oxygen, Eg(eV)**
4.86	3	2.263	2.27	2.354
5.35	4	2.132	2.251	2.32
5.8	5	1.997	2.073	2.291
6.5	7	1.916	1.981	2.264
6.8	8	1.822	1.891	2.213
7.3	10	1.814	1.887	2.211
7.7	12	1.806	1.879	2.198
8.2	14	1.797	1.871	2.187
8.5	16	1.792	1.86	2.156
8.7	17	1.79	1.854	2.114
8.8	18	1.693	1.824	2.046
9.2	20	1.637	1.816	2.029
9.7	24	1.582	1.799	2.011
11.2	36	1.528	1.781	1.987
11.9	44	1.513	1.766	1.975

Chapter Three

Results and Discussion

First, we considered a three-atom dot with and without hydrogen and oxygen at the surface. The effective size is ≈ 4.86 A^0 . This gives an energy gap of 2.263 eV with out any passivation and 2.27 eV with hydrogen passivation and 2.354 eV with oxygen. For a four-atom dot similarly the effective size is ≈ 5.35 A^0 and the energy gap with no passivation was 2.132 eV and 2.251 eV with hydrogen passivation and 2.32eV with oxygen.

For a five atom, dots with tetrahedral arrangement joined by a single bond 60^0 bond angles with out and with hydrogen atoms at the surface. The supper cell size chosen between 5.5 and 10.0, which is much higher, compare to that of the tunneling length (1.5 to 2.0 A^0) of electron as a result the interaction between two clusters is ignored. This gave an energy gap ≈ 1.997 eV without hydrogen atoms at the surface. In each case we kept the fixed bond length l = 5.43 A^0 between two silicon atoms to check if there is any change in gap from the spectrum of the energy eigen values in the presence of hydrogen. We have taken the value of the cut of 5 Ryd that corresponds to the n_j values running from -2 to +2. The corresponding G_j's are running from $G_j = \frac{-2\pi n_j}{l_j}$ to $G_j = \frac{+2\pi n_j}{l_j}$ etc; where n_j's are integers and G_j is reciprocal vector (where j's are x, y, and z). The dimension of the Hamiltonian matrix

is 125*125. We find the gap energy simply by counting the level occupation starting from the ground state. In this method, we have only four valence electrons associated with each silicon atom and for an N atom dot there is 4N number of electron. We fill the states by putting 2 electrons in each state until all valence electrons in each state until all valence electrons are exhausted. The difference in energy between the highest filled states (HOMO) and the lowest unfilled state (LUMO) states determine the gap energy. The basic features of the energy spectrum are dominated mainly by the large value of the kinetic energy than the rather weak pseudopotential.

For 5 atom dots with free surface the total number valence electron are 20 and 10 energy levels starting from the ground state (with double occupancies in each level) are required to fit all 20 electrons. The energy difference between the 10^{th} and the 11^{th} level is identified as the gap energy. Similarly, for 8 atom cluster the difference between the 16^{th} and the 17^{th} level gives the gap energy, for 17 atom cluster gap energy comes from the difference between the 34^{th} and 35^{th} level and for 18 atom cluster gap energy comes from the difference between the 36^{th} and the 37^{th} level .As we passivate the surface of 5 atom dot with hydrogen i.e. Si_5H_{12}, the occupied number of levels are 16 and the gap emerges between 16^{th} and 17^{th} levels.

Now we examine the eight-atom dot following a similar procedure. In this case each atoms are joined by a single length an appropriate dihedral angle (90^0) with out and with hydrogen atoms at the surface and found energy gap ≈ 1.82 eV with

hydrogen and ≈ 1.89eV with hydrogen at the surface. In each case we kept the fixed bond length a =4.0A^0 between two silicon atoms to check if there is any change in the gap from the spectrum of the energy eigen values due to hydrogen. We have taken the value of the cut of energy 5 Ryd that corresponds to the n_j values running from -2 to +2 and a matrix size is 125*125. A similar energy spectrum dominated by the kinetic energy was obtained. This was also found for the seventeen and eighteen atom clusters with lifting of degeneracy's more pronounced as we approach to large dots.

To see the behavior of the combination of two eight-atom cluster and the effect of an additional atom in the 16-atom dot we consider a seventeen-atom cluster. This structure is considered with four tetrahedral arranged nearest neighbors joined by a single bond (60^0-bond angle) and twelve next nearest neighbors (connected by single bond) and twelve next neighbors (connected by single bond) at the face centers without and with hydrogen atom at the surface. This gave an energy gap ≈ 1.79 eV without hydrogen and ≈ 1.85 eV with hydrogen at the surface .In each case we kept the fixed cell size l =3.2^0 between two silicon atoms to check if there is any change in the gap from the spectrum of the energy eigenvalues. We have taken the value of the cut of energy 5 Ryd that corresponds to the nj values running from -2 to +2 and a matrix size 125*125 is obtained.

Finally, an eight-atom cluster using the cubic cell with eight corner atoms, six face centered atoms and four atoms from the other sub-lattice entirely included

with in it without and with hydrogen atoms at the surface. An energy gap ≈ 1.693 eV with out hydrogen and ≈ 1.824 eV with hydrogen at the surface is observed .In each case we kept the fixed size cell $l = 3.0A^0$ between two silicon atoms to check if there is any change in the gap from the spectrum of the energy eigenvalues. We have taken the value of the cut of energy 5 Ryd which corresponds to the n_j values running from -2 to +2 and a matrix size 125*125 is obtained.

The table below presents our results for the gap energy as a function of the dot size, a detail comparison of our simulation with other calculation using effective mass approximations.

Table 2.5. Our results for the gap energy as a function of the dot size

Effective Size d (A^0)	Number Of Atoms Per Dots	TB:With Out Hydrogen	TB:With Hydrogen	Our result with Out Hydrogen	Our result With Hydrogen
4.86	3	2.269	2.278	2.27	2.27
5.35	4	2.211	2.229	2.132	2.251
5.8	5	2.042	2.109	1.997	2.073
6.5	7	2.029	2.094	1.916	1.981
6.8	8	1.879	1.938	1.822	1.891
7.3	10	1.875	1.929	1.814	1.887
7.7	12	1.87	1.919	1.806	1.879
8.2	14	1.868	1.913	1.797	1.871
8.5	16	1.863	1.908	1.792	1.86
8.7	17	1.86	1.901	1.79	1.854
8.8	18	1.729	1.847	1.693	1.824
9.2	20	1.717	1.836	1.637	1.816
9.7	24	1.639	1.811	1.582	1.799
11.2	36	1.591	1.789	1.528	1.781
11.9	44	1.521	1.773	1.513	1.766

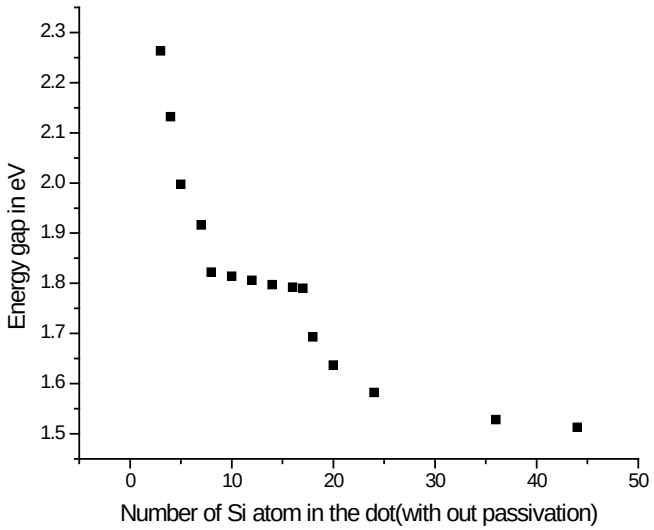

Figure 3.1. Plot of number of atom in the dot verses HOMO-LUMO energy gap value with out any passivation

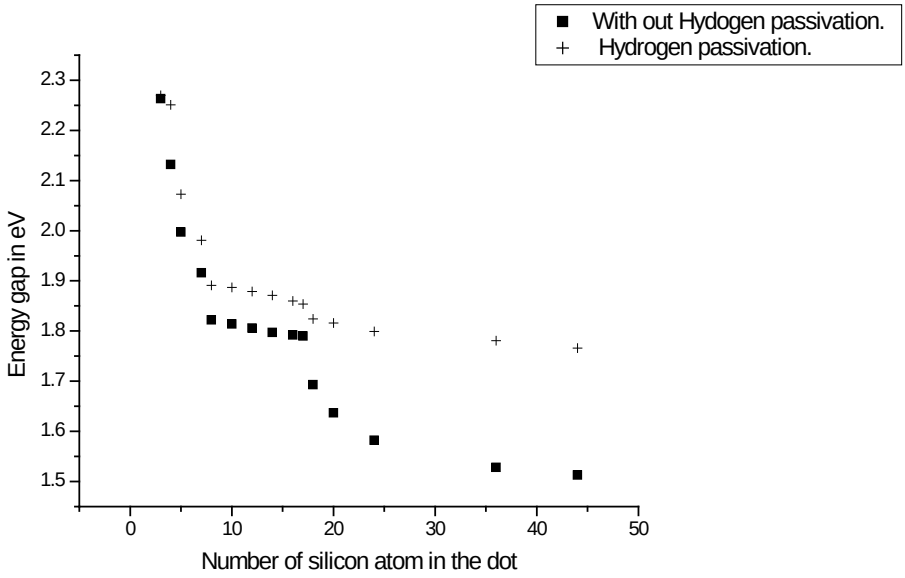

Figure 3.2. Plot of number of silicon atoms in the dot verses HOMO-LUMO energy gap value with and without hydrogen passivation.

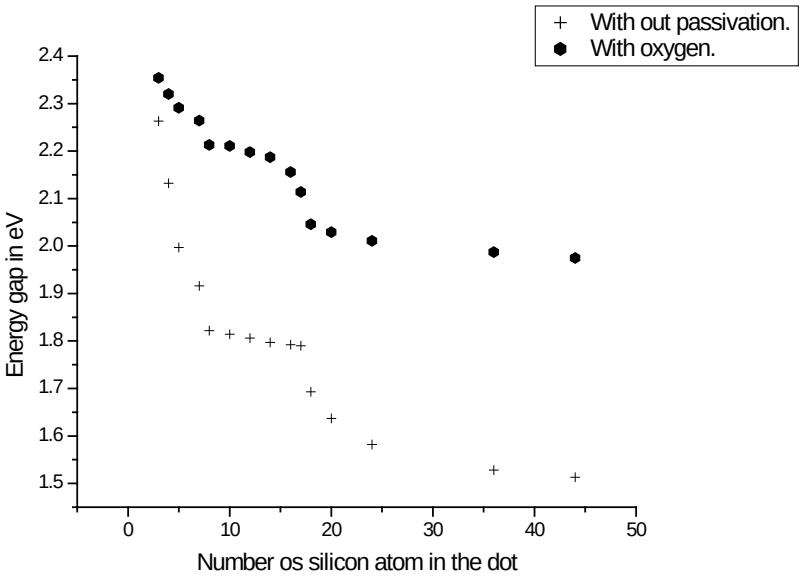

Figure 3.3. Plot of number of silicon atoms in the dot verses HOMO-LUMO energy gap value with and without oxygen passivation.

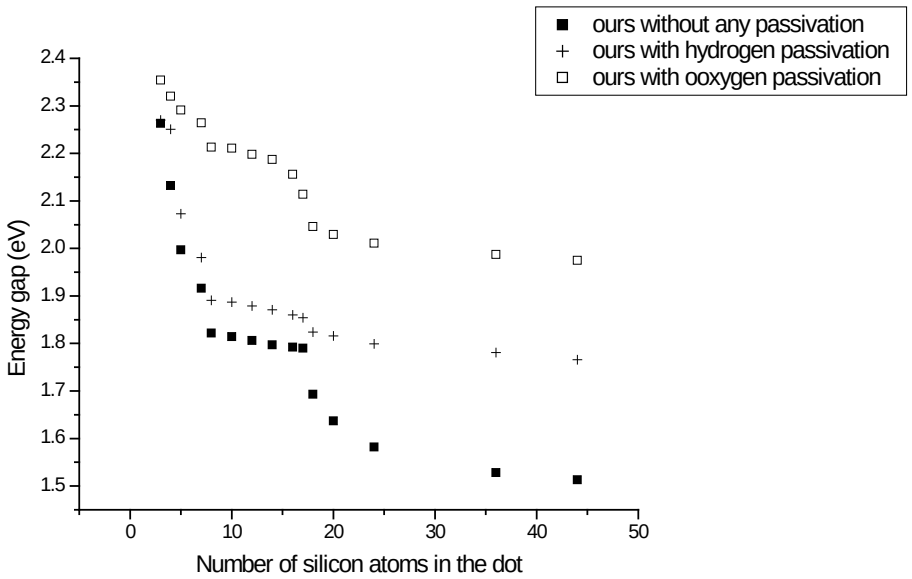

Figure 3.4. Plot of number of silicon atoms in the dot verses HOMO-LUMO energy gap value without any passivation, with hydrogen and with oxygen passivation.

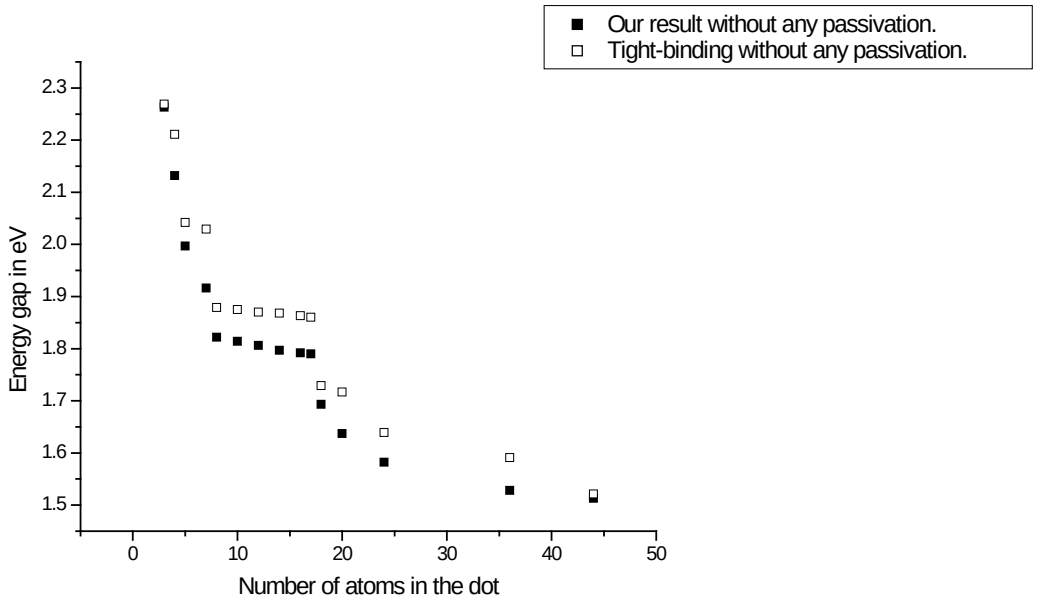

Figure 3.5. Plot of number of silicon atoms in the dot verses HOMO-LUMO energy gap value without passivation (our result and tight binding)

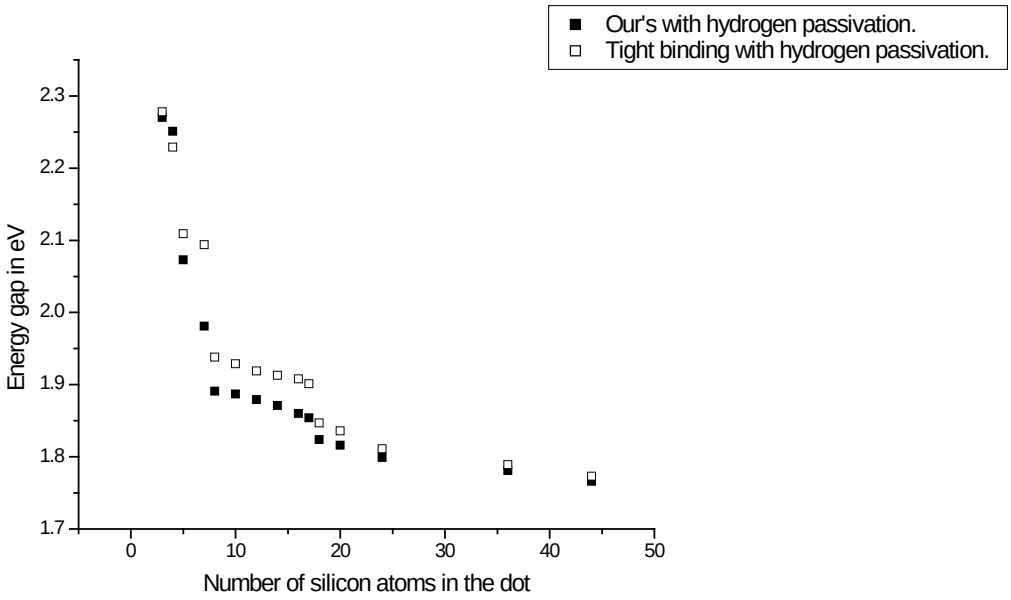

Figure 3.6. Plot of number of silicon atoms in the dot verses HOMO-LUMO energy gap value with hydrogen passivation (tight binding and ours).

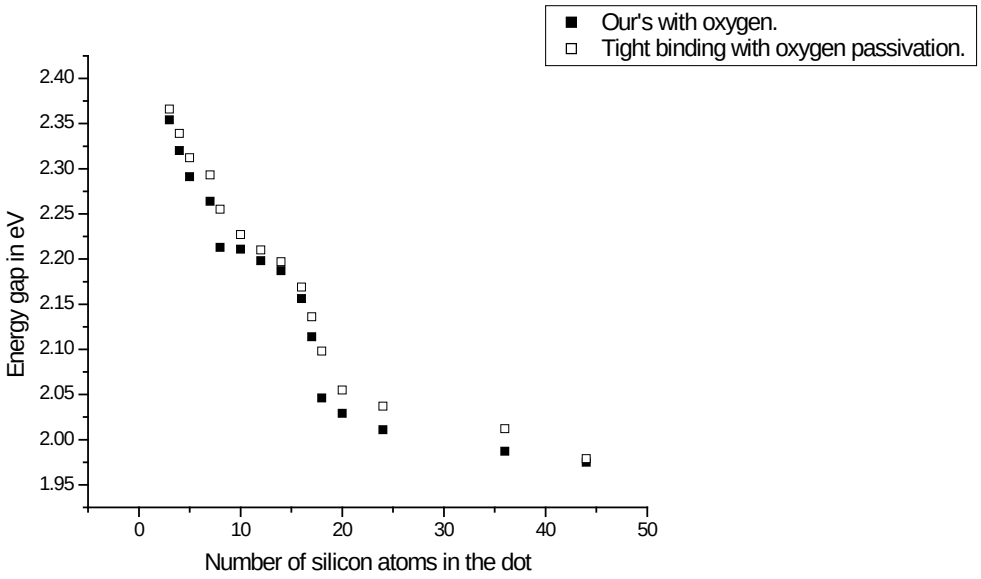

Figure 3.7. Plot of number of silicon atoms in the dot verses HOMO-LUMO energy gap value with oxygen passivation (tight binding and ours).

Chapter Four

Summary and Conclusion

To calculate electronic structure of silicon quantum dots of different sizes with different atoms and to examine the quantum size effects on gap energy we have used the empirical pseudo potential method. The role of multi-band coupling is neglected in the present treatment. Our results show that the gap energy increases as the size of the dot decreases implies the stronger confinement for smaller dots, which is conformity with recent experimental observations. This result is also in conformity with the earlier computer simulation result of Wang and Zunger. We also find an enhancement of the gap energy when the surface of the dot is passivated with the hydrogen atoms incorporating proper hydrogen pseudopotential. The most interesting and remarkable result we find for the HOMO LUMO gap energy as we vary the size of the dot size plays a crucial role with out any adjustable parameters in the simulation. We have observed that the change in the energy gap on passivation as a function of the dot size is more prominent for larger dots. This may be due to change in the number of hydrogen atoms at the surface, which has stronger effect near the gap states of the dot. Hydrogen passivation of the relaxed cluster eliminates most of the remnant dangling bonds but no appreciable effect on the defect states. With

hydrogen passivation, the localized dangling bond states are eliminated resulting in a wide energy gap.

We compare our data for the gap energy with Zunger and others, which is very close to the earlier observation under linear mapping of the size with the number of atoms in the dot.

References

[1] G.G .Qin and V.J.LI Phys. Rev. B 68.085309(2003)

[2] Lei Liv.C.S Jayanthi and Shi-Yu Wu J. of Applied Physics **90** , 8-15 Oct.(2001).

[3] Md.N.Islam and S. Kumar J.of Appl Phys.**93 ,**3 Feb. (2003).

[4] C.N.R Rao, A.Muler A.K. Cheetah the Chemistry of Nanomaterials **1**

Jan.(2003).

[5] Won Chel (HoI Chun Keun Kim and Eun Kyu Kim) J. phys.**36,** 23-28

,Jan.(2000) .

[6] C.N.R Rao.Amuler, A.K Cheetram The Chemistry of Nanomaterials **2**

[7] M.D. Mason, D.J.sirbuly P.J. Carson and S.K Buratto jour.of chemical phys. **14** may

(2001).

[8] S. K. Ghoshal ,As. J.Spect.7(2003) 49-68

[9] Mashiko Nishioa published journal 21 February 2006

[10] S.R.W and X.G.gong the J. of chemical phys. 122.17+311(2005).

[11] Neil W. Ashcroft, N. David Mermin, (1976).

[12] L. VasilieV, J.R.Chelikowsky, and R. M. Martin, phys.ReV.B 65,121302 (2002)